Contents lists available at ScienceDirect

Regenerative Therapy

Original Article

Mesenchymal stem cells derived from the fibrotic tissue of atrophic nonunion or the bone marrow of iliac crest: A donor-matched comparison

Feng Shen, Hao Xiao, Qiang Shi*

Department of Orthopaedics, The Affiliated Changsha Central Hospital, Hengyang Medical School, University of South China, Changsha, 410018, Hunan, People's Republic of China

ABSTRACT

Purpose: Atrophic nonunion is one of the most difficult complications of fracture. The cellular factors that contribute to atrophic nonunion are poorly understood, and mesenchymal stem cells (MSCs) are recognized as the key contributor to bone formation. This study aimed to characterize the MSCs isolated from the fibrotic tissue of atrophic nonunion (AN-MSCs) from the perspective of proliferation, differentiation potential, senescence, and paracrine function.

Methods: Human atrophic fibrotic tissue was obtained from four donors aged 29–37 for isolating AN-MSCs, and donor-matched bone marrow acquired from the iliac crest for isolating MSCs (IC-MSCs) as control. The AN-MSCs or IC-MSCs in passage 3 were applied for the following evaluations. The surface markers expressed on the two cells were evaluated using flow cytometry. The proliferation of the two cells for up to 11 days was comparatively investigated. After osteogenic, chondrogenic, or adipogenic induction, multi-lineage differentiation of AN-MSCs or IC-MSCs was comparatively evaluated using lineage-specific stains and lineage-specific gene expression. Enzyme-linked immunosorbent assay (ELISA) assessment was applied to evaluate the paracrine function of AN-MSCs or IC-MSCs. Cellular senescence of AN-MSCs or IC-MSCs was evaluated using senescence-associated β-galactosidase (SA-β-gal) staining.

Results: AN-MSCs or IC-MSCs from the four donors showed morphologic and immunophenotypic characteristics of MSCs, with the expression of MSCs markers and negative expression of hematopoietic markers. In general, AN-MSCs showed similar proliferation and adipogenic capacity with IC-MSCs. In contrast, IC-MSCs showed significantly higher osteogenic and chondrogenic capacity compared to AN-MSCs. Moreover, the culture medium of IC-MSCs contains significantly higher levels of VEGF, TGF-β1, PDGF-BB, and IGF-1 than the culture medium of AN-MSCs. Lastly, the AN-MSCs are more prone to cellular senescence than the IC-MSCs.

Conclusions: In-vitro, AN-MSCs were similar to IC-MSCs in proliferation and adipogenic capacity, but inferior to IC-MSCs in osteogenic and chondrogenic capacity, paracrine function, and anti-senescence.

1. Introduction

Fracture nonunion occurs in approximately 5–10% of long bone fractures [1], which is one of the most difficult complications of fracture, and decreased the function and life quality of the patient [2,3]. To effectively treat fracture nonunion, the surgeon and scientists classified it into either hypertrophic or atrophic according to characteristic radiological features [4]. The hypertrophic nonunion is mainly caused by inadequate mechanical fixation, as characterized by lots of hypertrophic callus forming at the fracture site with

* Corresponding author. The Affiliated Changsha Central Hospital, Hengyang Medical School, University of South China, No. 161, Shaoshan Road, Yuhua District, Changsha, 410018, People's Republic of China.
E-mail address: shiqiang542@126.com (Q. Shi).

Peer review under responsibility of the Japanese Society for Regenerative Medicine.

ubiquitous blood, oxygen and nutrient supply [5]. Thus, the treatment of hypertrophic nonunion is directed toward stabilization of the fracture. In the case of atrophic nonunion, no callus is formed at the fracture site [2,5], and the contributing factor and pathophysiology of developing atrophic nonunion remain poorly understood.

According to literatures, the contributing factors leading to atrophic nonunion can be classified into patient-specific factors or injury severities and operations. Among them, patient-specific factors, such as age, gender, smoking, diabetes, hormone disorders, and genetic factors, are widely accepted to influence atrophic nonunion [6,7]. In addition, injury severities and operation, including the bone loss at the fracture site, extensive periosteum damage, infection, and open fractures, are closely related to the quality and speed of bone formation at the fracture site [6,7]. Regarding these risk factors associated with developing atrophic nonunion, no reliable measure was available for predicting them. Thus, surgeons paid more attention to elucidating the underlying pathophysiology of developing atrophic nonunion.

Previously, poor vascularization was considered a cause of atrophic nonunion, which was supported by a study that arterial occlusion in the ipsilateral extremity was associated with a higher rate of delayed union or nonunion in tibia fractures [8]. However, this conception has been challenged by several literatures that found significant vascularity in the fibrotic tissue of atrophic nonunion [9,10]. Currently, the conception that the atrophic tissue is avascular has been proven to be incorrect. Another conception pointed out that the development of atrophic nonunion mainly resulted from the lack of regenerative cells in the fibrotic tissue. This was supported by several studies [11,12], in which the percutaneous injection of culture-expanded bone marrow-derived mesenchymal stem cells (BM-MSCs) could enhance fracture healing in nonunion. However, some studies confirmed that mesenchymal stem cells (MSCs) are located at the fibrotic tissue of atrophic nonunion and show similar quantities to the MSCs in the iliac crest, but they presented in a state of reduced osteogenic potential and increased cell senescence [13,14]. This conception was supported by M Orth et al.' study, in which they delivered BMP-2 into the site of atrophic nonunion to stimulate the osteogenic differentiation of stem cells, and then promoted the healing of murine atrophic nonunion [15].

Whether the MSCs showing reduced biological activities at the site of atrophic nonunion is the primary cause of developing atrophic nonunion remains an unsolved controversy and warrants further study. In this study, we comparatively evaluated the proliferation, multipotentiality, senescence, and paracrine function of MSCs isolated from the fibrotic tissue of atrophic nonunion (AN-MSCs) or the bone marrow of iliac crest (IC-MSCs) (Fig. 1).

2. Materials and methods

2.1. Ethical approval

Ethical approval was attained from the Medical Ethics Committee of Xiangya Hospital (No. 20211207-5) for the harvesting of fibrotic tissue from the atrophic nonunion site or bone marrow from the iliac crest. The recruited patients gave informed consent and research was performed in compliance with the Helsinki Declaration.

2.2. Patient recruitment and tissue collection

The participants were recruited at the Xiangya Hospital, Central South University, Changsha, Hunan, China, who were patients admitted for treatment of atrophic nonunion in either the upper or lower extremity. In total, four patients suffering from atrophic nonunion were recruited, who were addressed with excision of atrophic fibrotic tissue, compression plating or nailing exchange, then autogenous iliac bone autograft. The characteristics of the four patients are listed in Table 1. During the operation, the atrophic

Table 1
Characteristics of the recruited patients.

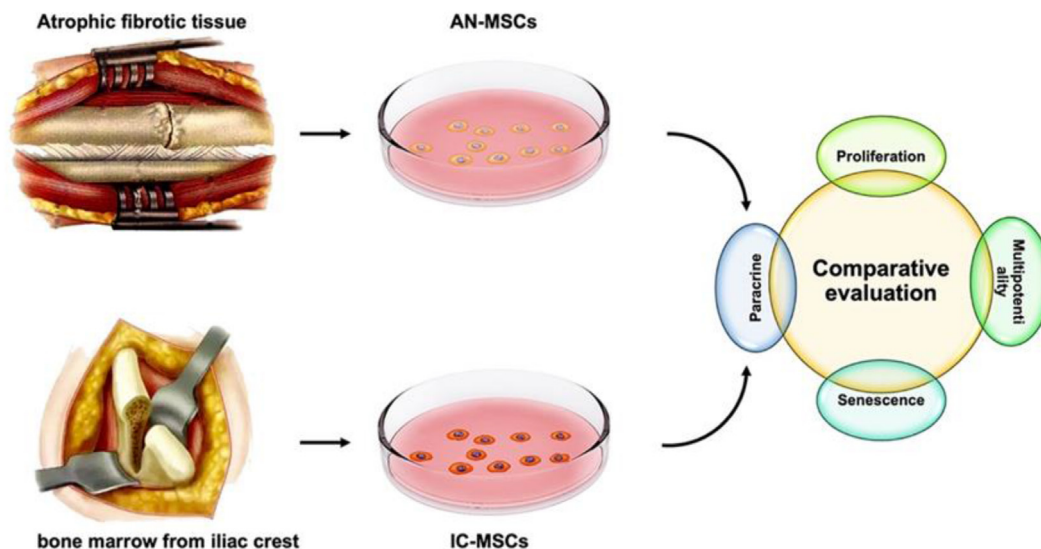| Patient	ID	Age (Years)	Gender	Fracture duration (Months)	Site
1	1,775,581	29	Male	16	Left tibia
2	1,430,310	34	Male	36	Right femur
3	1,723,638	37	Male	18	Right radius
4	1,752,945	35	Male	12	Right femur

Fig. 1. Schematic diagram showing the study design, MSCs were isolated from the fibrotic tissue of atrophic nonunion (AN-MSCs) or the bone marrow of iliac crest (IC-MSCs), and then comparative evaluation of their proliferation, multipotentiality, senescence, and paracrine function.

Table 2
Primer sequences utilized for qRT-PCR gene expression analysis.

Gene	Primer sequence		Species
RUNX2	Forward primer	5′- CGCCTCACAAACAACCACAG -3′	human
	Reverse primer	5′- GGTAGTGACCTGCGGAGATT -3′	
BGLAP	Forward primer	CACTCCTCGCCCTATTGGC	human
	Reverse primer	CCCTCCTGCTTGGACACAAAG	
SOX9	Forward primer	5′-TGGGCAAGCTCTGGAGACTTC-3′	human
	Reverse primer	5′-ATCCGGGTGGTCCTTCTTGTG-3′	
ACAN	Forward primer	5′-GCCTATCAGGACAAGGTCTCAC-3′	human
	Reverse primer	5′-ATGGCTCTGTAATGGAACACGA-3′	
PPARγ	Forward primer	5′-CCGTGGCCGCAGATTTGA-3′	human
	Reverse primer	5′-AGATCCACGGAGCTGATCCC-3′	
LPL	Forward primer	5′-ACGGCATGTGAATTCTGTGA-3′	human
	Reverse primer	5′-GGATGTGCTATTTGGCCACT-3′	
GAPDH	Forward primer	5′- GGAGTCAACGGATTTGGTCGT -3′	human
	Reverse primer	5′- GCTTCCCGTTCTCAGCCTTGA -3′	

RUNX2: runt-related transcription factor 2; BGLAP: bone γ-carboxyglutamate protein; SOX9: sex-determining region Y-box 9; ACAN: Aggrecan; PPARγ: peroxisome proliferator-activated receptor γ; LPL: lipoprotein lipase; GAPDH glyceraldehyde-3-phosphate dehydrogenase.

fibrotic tissue and the bone marrow from the iliac crest were collected for the following cell isolation.

2.3. Cells isolation

After atrophic fibrotic tissue was harvested from the center of the bone defect area, tissue was extensively washed with phosphate-buffered saline (PBS) and then minced aseptically using sterilized surgical scissors, followed by digestion with type I collagenase solution (0.1 mg/mL, Gibco, USA) for 2 h in a 37 °C water bath shaker. After filtration and centrifugation, the cells were washed with PBS and resuspended in a culture medium (BMHX-G101, Haixing Biosciences), and incubated at 37 °C, 5% CO2. In addition, bone marrow from the iliac crest was directly seeded into a cell culture plate and cultured in a culture medium (BMHX-G101, Haixing Biosciences) to isolate MSCs, as previously described [16]. When reached 70−80% confluence, cells were passaged.

2.4. Cell proliferation

Cell Counting Kit-8 (CCK-8) assay was used to evaluate the proliferation ability of AN-MSCs or IC-MSCs. Briefly, the two kinds of isolated cells at passage 3 were plated in a 96-well plate at 2.0×10^3 cells per well ($n = 4$) and incubated at 37 °C with 5% CO_2. At time points of 1, 3, 5, 7, and 9 days, the cells in each well were incubated with 10 μL of CCK-8 reagent and 100 μL serum-free medium for 2 h. The absorbance at 450 nm of the cell culture medium was recorded using a microplate reader (Varioskan LUX, Thermo, USA).

2.5. Flow cytometry

Flow cytometry analysis was used to evaluate the surface markers of the isolated AN-MSCs or IC-MSCs. Briefly, a total of 1×10^6 AN-MSCs or IC-MSCs at passage 3 from the four patients were, respectively, suspended in 100 μL phosphate-buffered saline (PBS) containing 10 μg/mL antibodies for MSC surface markers (CD73, CD90, and CD105) and hematopoietic surface markers (CD34 and CD45), and then incubated at 4 °C for 30 min. After being washed with PBS, these cells were resuspended in 500 μL of PBS for flow cytometry using a DxP Athena™ flow cytometry system (Cytek) and analyzed with FlowJo 10 software (Tree Star, USA).

2.6. In-vitro osteogenesis, chondrogenesis, and adipogenesis

AN-MSCs or IC-MSCs at passage 3 from four patients were cultured in culture medium (BMHX-G101, Haixing Biosciences) at 5000 cells/cm² in 6-well plates. When the cultured cells reached about 60% confluence, they were cultured with osteogenic induction medium (BMHX-D101, Haixing Biosciences), chondrogenic induction medium (BMHX-D203, Haixing Biosciences), or adipogenic induction medium (BMHX-D102, Haixing Biosciences). The culture medium was changed every 3 days. After 7-day culture, qRT-PCR was performed for evaluating the expression of osteogenic genes (RUNX2, BGLAP), chondrogenic genes (SOX9, ACAN), and adipogenic genes (PPARγ, LPL) in the cells. The primer sequences
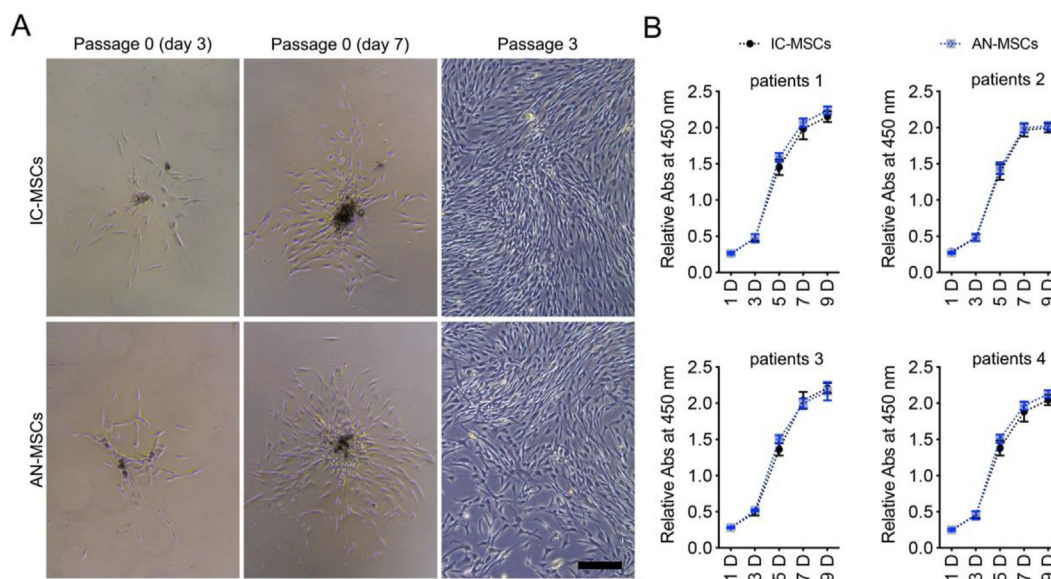

Fig. 2. (A) Morphology of MSCs isolated from the fibrotic tissue of atrophic nonunion (AN-MSCs) or the bone marrow of iliac crest (IC-MSCs). Bar = 100 μm. (B) The proliferation of AN-MSCs and IC-MSCs from four patients was determined by CCK-8 assay. Four samples were measured for each time point. The experiment was performed independently on the four patients.
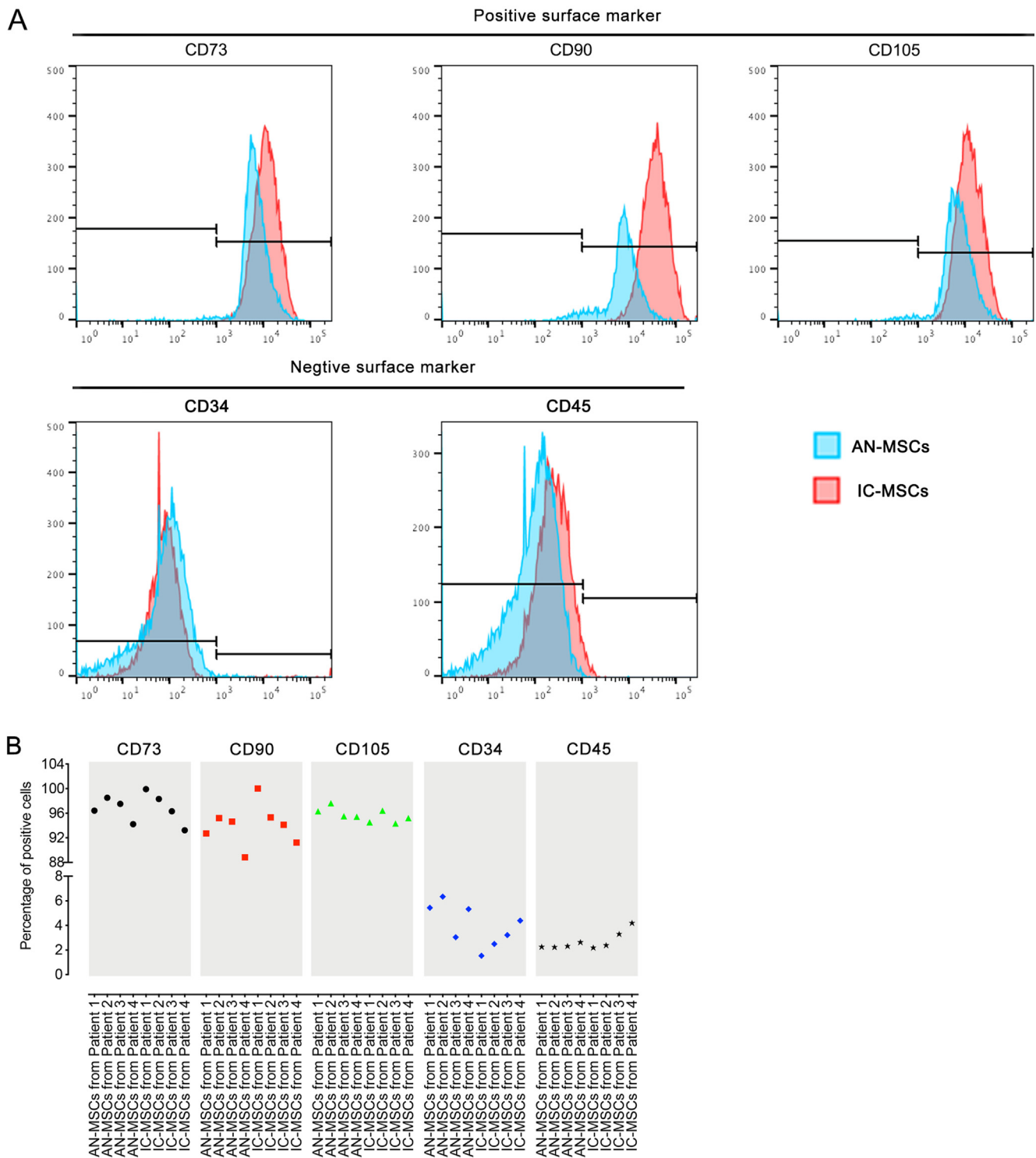
Fig. 3. (A) Representative histograms demonstrating positive and negative staining of AN-MSCs or IC-MSCs from a single patient. (B) Expression of surface markers in the AN-MSCs or the IC-MSCs isolated from the four patients.

were also listed in Table 2. In addition, immunofluorescence assay was performed for observing the RUNX2, SOX9, or PPARγ expression in the cells. After a 21-day culture, Alizarin Red, Alcian blue, and Oil red O staining assay was used for assessing the osteogenic differentiation, chondrogenic differentiation, and adipogenic differentiation of isolated cells.

2.7. In-vitro paracrine function

Previous literature indicated that the cytokines, such as VEGF, TGF-β1, PDGF-BB, and IGF-1, have been proven to regulate angiogenesis, cell migration, proliferation, and osteoblast differentiation [17]. Thus, ELISA assessment was applied to detect the conce-
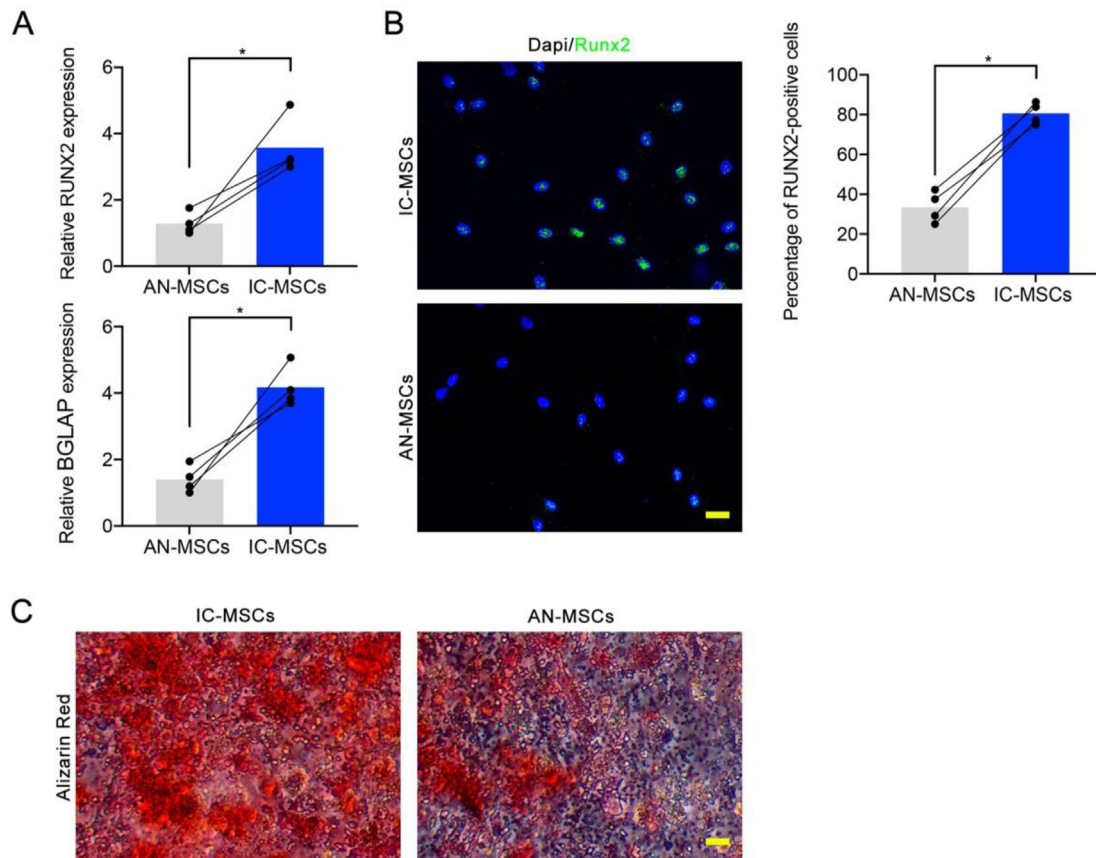
Fig. 4. Osteogenic differentiation of the AN-MSCs and the IC-MSCs in-vitro. (A) Osteogenic gene (Runx2, Bglap) expression compared between the AN-MSCs and the IC-MSCs. **P < 0.01. (B) Runx2 protein expression of the AN-MSCs or the IC-MSCs after 7 days of osteogenic induction. Bar = 15 μm. (C) Alizarin Red staining of the AN-MSCs or the IC-MSCs after culturing in an osteogenic medium for 21 days. Bar = 15 μm.

ntration of these cytokines in the culture medium of AN-MSCs (AN-MSCs-CM) or IC-MSCs (IC-MSCs-CM) at passage 3 to evaluate the paracrine function of AN-MSCs or IC-MSCs. In brief, 1.5 mL of AN-MSCs-CM or IC-MSCs-CM was combined with 100 μL of protease inhibitor, and then measured the above-mentioned cytokines using human enzyme-linked immunosorbent assay (ELISA) kits (Cusabio, China).

2.8. Cellular senescence

Cellular senescence of AN-MSCs or IC-MSCs was evaluated using senescence-associated β-galactosidase (SA-β-gal) staining kit (Beyotime, Shanghai, China). AN-MSCs or IC-MSCs at passage 3 were seeded in a 6-well plate at 2.0×10^6 cells per well. When cells reached 90% confluence, the medium was discarded, and the cells were rinsed with PBS. After these cells were fixed with 4% (w/v) paraformaldehyde for 15 min, they were rinsed with PBS for a further three times. After 1 mL of working solution was added to the cells incubated at 37 °C overnight away from light, the senescent cells in each group (n = 4) were captured and mounted under an optical microscope.

2.9. Statistical analysis

SPSS version 25 (IBM, USA) was used for statistical analysis, and P < 0.05 was considered significant, while GraphPad Prism version 9.00 (GraphPad Software Inc., La Jolla, CA, USA) was used to generate all graphs. All quantitative data are presented as mean ± standard deviation. The comparison between the two groups was analyzed using a paired Student's t-test.

3. Results

3.1. Morphology and proliferation of AN-MSCs or IC-MSCs

After the primary culture of 3 days, some cells adhered to the culture plate and formed several colonies with spindle-shaped or round-shaped colonies (Fig. 2A). After the primary culture of 7 days, the colonies of AN-MSCs or IC-MSCs were gradually enlarged and presented a similar diameter (Fig. 2A). At passage 3, both AN-MSCs and IC-MSCs showed a homogeneous spindle-shaped morphology (Fig. 2A). As shown in Fig. 2B, the CCK-8 assay showed that the AN-MSCs or the IC-MSCs from the four patients at passage 3 proliferated similarly without significant difference.

3.2. Surface marker of AN-MSCs or IC-MSCs

According to the criteria for defining MSCs proposed by the International Society for Cellular Therapy (ISCT) [18], the positive surface markers (CD73, CD90, and CD105) and negative surface markers (CD34 and CD45) were selected to analyze the isolated AN-MSCs or IC-MSCs by flow cytometric analysis. As shown in Fig. 3, the isolated AN-MSCs or IC-MSCs at passage 3 were positive for MSC-special markers (CD73, CD90, and CD105), and negative hematopoietic markers (CD34 and CD45).
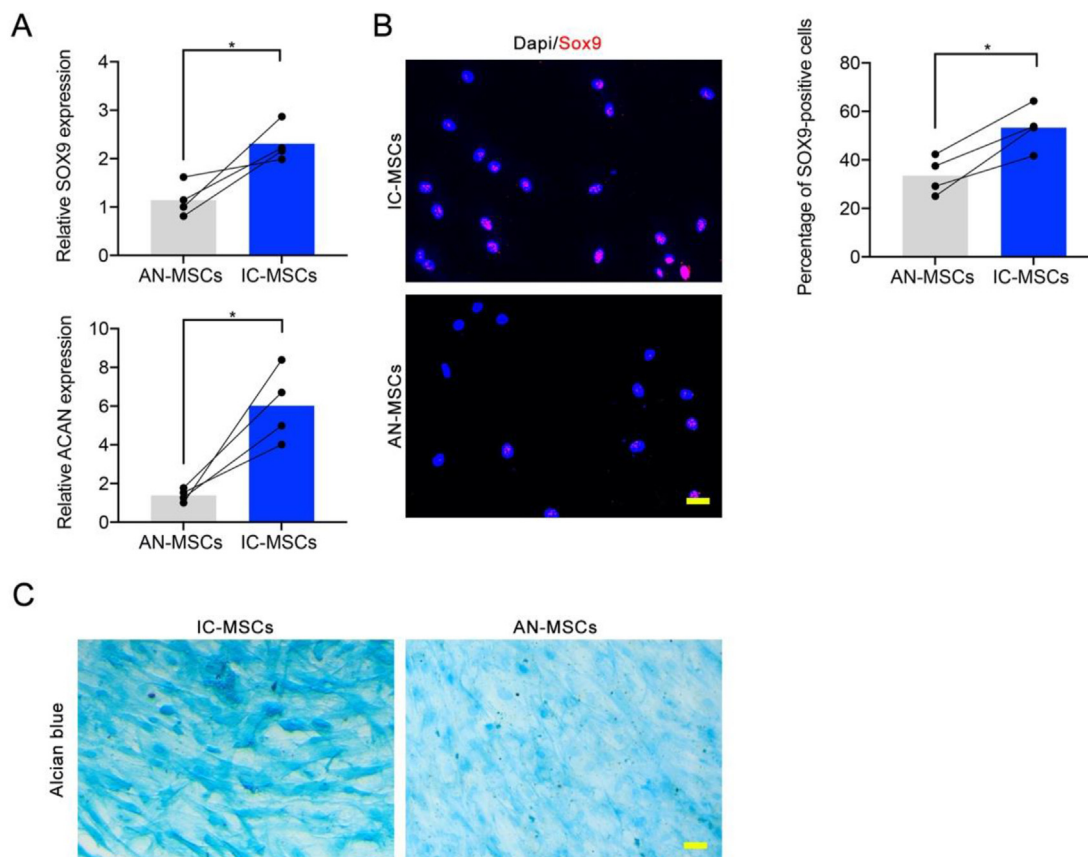
Fig. 5. Chondrogenic differentiation of the AN-MSCs and the IC-MSCs in-vitro. (A) Chondrogenic gene (Sox9, Acan) expression was compared between the AN-MSCs and the IC-MSCs. *P < 0.05, **P < 0.01. (B) Sox9 protein expression of the AN-MSCs or the IC-MSCs after 7 days of chondrogenic induction. Bar = 15 μm. (C) Alcian blue staining of the AN-MSCs or the IC-MSCs after culturing in a chondrogenic medium. Bar = 15 μm.

3.3. Multi-lineage differentiation

After culturing in an osteogenic medium for 7 days, the AN-MSCs expressed significantly lower expression of RUNX2 and BGLAP genes compared with the IC-MSCs (P < 0.05 for all) (Fig. 4A). In addition, under osteogenic induction, significantly more IC-MSCs are positive for RUNX2 protein expression (P < 0.05) (Fig. 4B). At 21 days of osteogenic induction, Alizarin red stained images showed the calcium nodules in the IC-MSCs were significantly more when compared with the AN-MSCs (Fig. 4C).

Similarly, after culturing the AN-MSCs in a chondrogenic medium for 7 days, they expressed significantly lower expression of SOX9 and ACAN genes compared with the IC-MSCs (P < 0.05 for all) (Fig. 5A). Additionally, under chondrogenic induction, the SOX9 protein in the IC-MSCs expressed significantly more when compared with AN-MSCs (P < 0.05) (Fig. 5B). After 21 days of chondrogenic induction, there was more glycosaminoglycan deposition found around the IC-MSCs compared with the AN-MSCs under Alcian blue staining (Fig. 5C).

As for adipogenic differentiation, the AN-MSCs and the IC-MSCs cultured within adipogenic induced medium expressed a similar level of PPARγ and LPL (Fig. 6A). In addition, immunofluorescence staining showed that the expression of PPARγ protein was similar in the AN-MSCs and the IC-MSCs (Fig. 6B). After 21 days of adipogenic induction, Oil red O staining showed that the presence of intracytoplasmic lipid droplets was similar in the AN-MSCs and the IC-MSCs (Fig. 6C).

3.4. Concentration of VEGF, TGF-β1, PDGF-BB and IGF-1 in the culture medium

The concentration of the VEGF, TGF-β1, PDGF-BB, and IGF-1, released by the AN-MSCs or the IC-MSCs into a culture medium, was quantified using ELISA analysis. AN-MSCs-CM and IC-MSCs-CM contained VEGF, at a concentration of 68.41 ± 30.51 pg/mL and 213.90 ± 63.18 pg/mL, respectively (P < 0.05) (Table 3). TGF-β1, PDGF-BB, and IGF-1 were not identified in the AN-MSCs-CM, while the concentrations of TGF-β1, PDGF-BB, and IGF-1 in the IC-MSCs-CM were 5.75 ± 1.13 ng/mL, 33.98 ± 15.91 pg/mL, 21.27 ± 4.69 ng/mL, respectively (Table 3).

3.5. Phenotypic character of cellular senescence

We investigated the phenotypic character of cellular senescence by measuring the activation of SA-β-gal. We observed that nearly 71.26% of the AN-MSCs were stained positive for SA-β-gal (blue-green) (Fig. 7A), whereas only about 32.11% of IC-MSCs were stained positive (Fig. 7B). These findings suggest that the AN-MSCs are more prone to cellular senescence than the IC-MSCs.

4. Discussion

Atrophic nonunion was an urgent public health problem with detrimental socioeconomic costs and productivity losses. The progression of atrophic nonunion was influenced by multiple
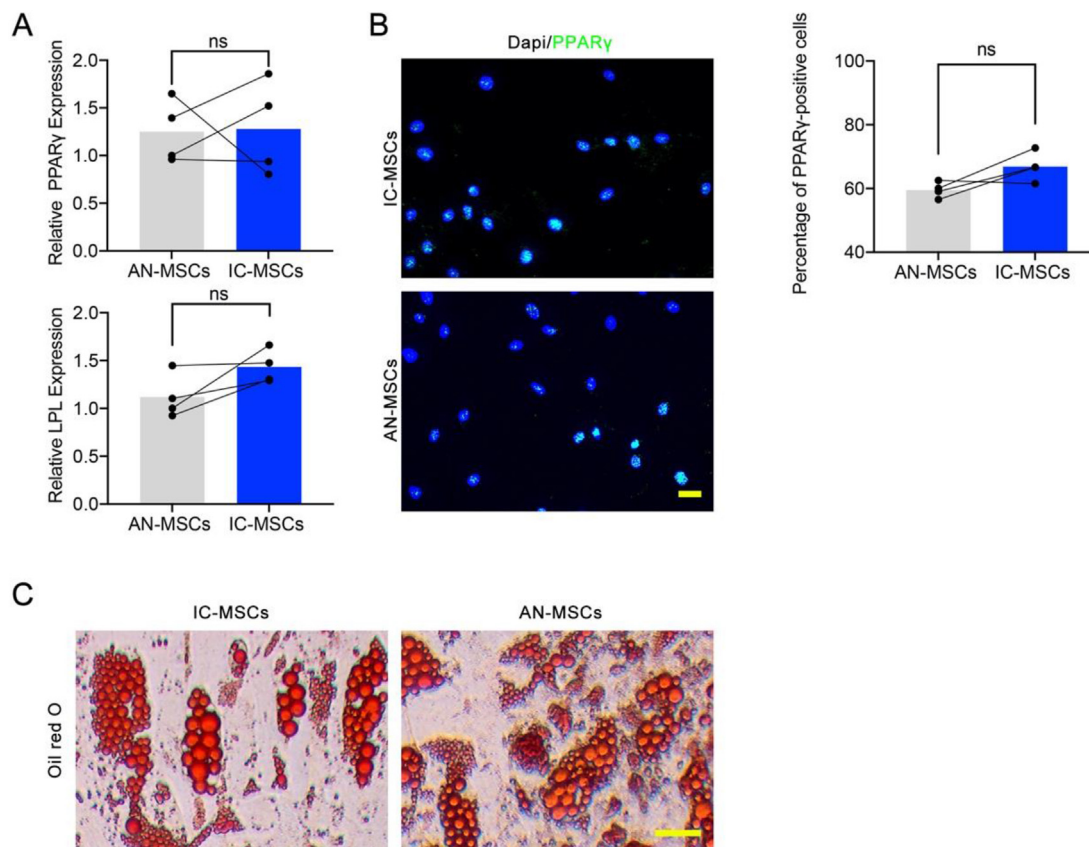
Fig. 6. Adipogenic differentiation of the AN-MSCs and the IC-MSCs in-vitro. (A) adipogenic gene (PPARγ and LPL) expression compared between the AN-MSCs and the IC-MSCs. "ns" means no significance. (B) PPARγ protein expression of the AN-MSCs and the IC-MSCs after 7 days of adipogenic induction. Bar = 15 μm. (C) Oil Red O staining of the AN-MSCs or the IC-MSCs after culturing in adipogenic medium. Intracytoplasmic lipid droplets were seen in the adipogenic-induced medium. Bar = 15 μm.

pathophysiological factors, including patient state, injury severities, and operation time, thus the treatment of fracture nonunion remains a challenge [19]. With the improved understanding of its pathophysiology, the treatment strategies of fracture nonunion have been evaluated from prolonged immobilization in the 1950s to the modern techniques of biological therapy [20,21].

As for the understanding of atrophic nonunion, the macroscopic appearance of atrophic nonunion was firstly described, as characterized by bony sclerosis of fracture ends, complete obliteration of medullary canal, and lots of fibrotic tissue interposition between fracture ends [8,19]. Elucidating the macroscopic appearances could serve as a powerful visual marker, guiding surgeons with fibrotic tissue removal and fracture end freshening. Right after, researchers and surgeons found that the fibrotic tissues of atrophic nonunion are histologically a mixture of fibrous, cartilaginous, and connective tissues, low cellular density, and full of whilst fibroblast-like cells [22,23,13]. More seriously, the fibrotic tissues of atrophic nonunion were lack of viable osteocytes and osteoclasts [13]. Interestingly, the fibrotic tissue was found to contain regenerative cells positive for MSCs-related markers and negative for hematopoietic markers. Moreover, these regenerative cells were capable of

differentiating into osteoblastic, chondrogenic, and adipogenic lineages [13,24,14]. Injected platelet-rich plasma or external low-intensity pulsed ultrasound stimulation may directly regulate the biological activities of these regenerative cells, thus enhancing the repair of atrophic nonunion [25,26].

Toward these regenerative cells in the atrophic nonunion tissue, only a few studies evaluated and characterized its biological activities [14,27]. As for the proliferative capacity of MSCs isolated from nonunion tissue, there exists a dispute. Cuthbert et al. and Vallim et al. found the proliferative capacity of MSCs isolated from nonunion tissue to be comparable to that of BM-MSCs [27,24]. While Takahara S et al. found that the proliferative capacity of MSCs from nonunion tissue was found to have minimal decline following multiple passages [28]. Our results indicated that the AN-MSCs show similar proliferation to IC-MSCs. As for the multipotentiality of AN-MSCs, R J Cuthbert et al. only determined that the AN-MSCs were capable of differentiating into osteoblastic, chondrogenic, and adipogenic lineages [27]. While the multipotentiality difference between AN-MSCs and IC-MSCs has never been evaluated. Our in-vitro results indicated that the AN-MSCs at passage 3 showed lower ability to differentiate into osteoblastic and chondrogenic lineages than the IC-MSCs. In addition, the AN-MSCs showed a similar property of differentiating into adipogenic lineages with IC-MSCs.

Cell senescence has been found to impair the regenerative potential of MSCs [29]. Currently, no consensus has been reached on whether the rate of cell senescence was higher in the nonunion tissues than in the normal bone marrow. In Vallum et al.'s study, there is no difference in senescence rate between MSCs from nonunion tissue and BM-MSCs [24]. Whereas, Bajada et al. reported

Table 3
The levels of cytokines present in the AN-MSCs-CM or the IC-MSCs-CM.

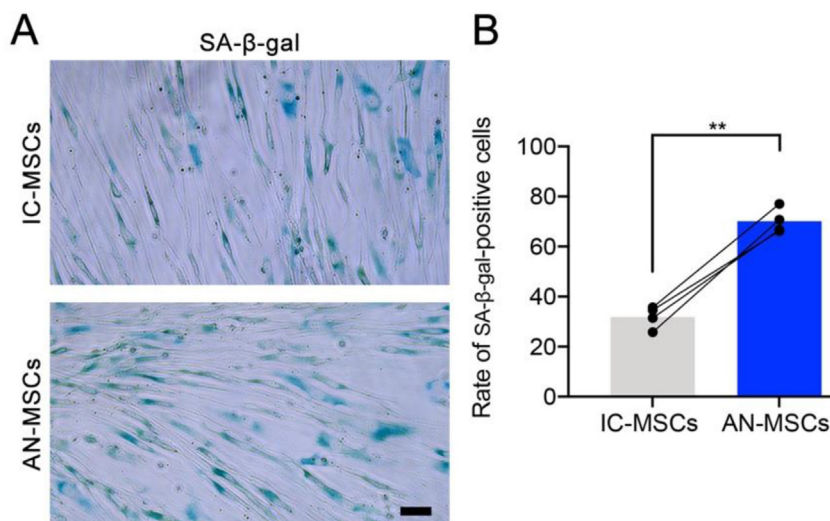| Cytokines	AN-MSCs-CM	IC-MSCs-CM
VEGF	68.41 ± 30.51 pg/mL	213.90 ± 63.18 pg/mL
TGF-β1	No detection	5.75 ± 1.13 ng/mL
PDGF-BB	No detection	33.98 ± 15.91 pg/mL
IGF-1	No detection	21.27 ± 4.69 ng/mL

Fig. 7. (A) the IC-MSCs or the AN-MSCs at passage 3 were stained for SA-β-gal. Bar = 10 μm. (B) Comparison of the rate of SA-β-gal positive cells in the IC-MSCs or the AN-MSCs at passage 3 from the four patients.

an increased proportion of MSCs senescence in nonunion tissue when compared with BM-MSC [13]. In our study, senescence-associated β-galactosidase staining showed that more AN-MSCs (Passage 3) showed a state of senescence when compared with the IC-MSCs (Passage 3) from the same patient. The results suggest that the occurrence of fracture nonunion may be associated with the MSCs in the atrophic nonunion showing a tendency of cell senescence.

Finally, ELISA assay was performed to understand AN-MSCs or IC-MSCs secreted cytokines associated with angiogenesis, cell migration, proliferation, and osteoblast differentiation in the culture medium. In a published literature [27], the culture medium of AN-MSCs had a negligible effect on in-vitro stimulating the human umbilical vein endothelial cells (HUVECs) forming tubes. Meanwhile, our in-vitro results determined that the content of VEGF (a cytokine closely associated with angiogenesis) in the culture medium of AN-MSCs was significantly lower than that of the IC-MSCs. Thus, we speculate that the MSCs in the atrophic nonunion tissue show a lower capability of secreting VEGF, thus influencing the angiogenesis at atrophic nonunion tissue. Similarly, the content of TGF-β1, PDGF-BB, and IGF-1 in the culture medium of AN-MSCs was significantly lower than that of the IC-MSCs. According to literature, TGF-β1, PDGF-BB, and IGF-1 are polyfunctional regulatory growth factors that function on MSC migration, osteoblastic and chondrogenic differentiation, and extracellular matrix (ECM) accumulation during bone formation [30–34]. This result is consistent with the limited cell proliferation and osteogenesis observed at the atrophic nonunion tissue [13].

This study exists several limitations. Firstly, only the VEGF, TGF-β1, PDGF-BB, and IGF-1 were measured using ELISA assay to evaluate the paracrine function of isolated MSCs. Strictly speaking, proteome profiler human cytokine array should be performed to assess the differences in cytokines content between AN-MSCs-CM and IC-MSCs-CM [35]. Secondly, the number of MSCs in the atrophic nonunion tissue was not measured. Next step, we should use a flow cytometry-based method with special markers to measure the count of stem cells in the atrophic nonunion tissue [36]. Thus, we can give a definite answer about whether there are fewer MSCs located in the atrophic nonunion tissue. Thirdly, the multipotent-iality of AN-MSCs or IC-MSCs was evaluated in a cell culture plate. Recent literature indicated that three-dimensional culture systems have proven to be closer to in-vivo natural systems, thus proving to be a

useful tool for comparatively assessing the biological characteristics of different cell types [37]. In future studies, the multipotentiality between AN-MSCs and IC-MSCs should be evaluated in these three-dimensional culture systems. Fourthly, our results indicated that AN-MSCs exhibited similarities to IC-MSCs in terms of proliferation and adipogenicity, and showed inferior performance compared to IC-MSCs in osteogenic and chondrogenic capacity, paracrine function, and anti-senescence. Next step, RNA sequencing technique should be applied to further insight the mechanisms underlying these different properties between AN-MSCs and IC-MSCs. Despite these limitations, this study indicated that AN-MSCs showed lower multi-lineage differentiation, easier to cell senescence, and worse paracrine function than the IC-MSCs in-vitro.

5. Conclusions

In conclusion, our results showed the existence of MSCs in the fibrotic tissue of atrophic nonunion, at a similar proliferation capacity to MSCs isolated from the iliac crest, but showing a lower multipotentiality, easier to cell senescence, and worse paracrine function. The study may help us further understand the pathophysiology of developing atrophic nonunion.

Ethics approval

The authors are accountable for all aspects of the work in ensuring that questions related to the accuracy or integrity of any part of the work are appropriately investigated and resolved. All procedures complied with the Animals (Scientific Procedures) Act 1986 and received university ethical approval of Xiangya Hospital (20211207-5).

Consent to participate

All patients and their families gave their written informed consent to participate.

Consent for publication

All patients and their families gave their written informed consent for the publication of their individual data and identifying photographs.

Authors' contributions

(I) Conceptualization and Data curation: FS; (II) Funding acquisition: FS and QS; (III) Supervision: FS; (IV) Validationa: HX; (V) Writing − original draft: HX and QS; (VI) Writing − review & editing: FS and QS; (VII) Final approval of manuscript: All authors.

Funding

Availability of data and material

Not applicable.

Code availability

Not applicable.

Declaration competing of interest

The authors declare that they have no conflict of interest.

References

[1] Panteli M, Vun JSH, Pountos I, Jh A, Jones E, Giannoudis PV. Biological and molecular profile of fracture non-union tissue: a systematic review and an update on current insights. J Cell Mol Med 2022;26(3):601–23. https://doi.org/10.1111/jcmm.17096.
[2] Gómez-Barrena E, Rosset P, Lozano D, Stanovici J, Ermthaller C, Gerbhard F. Bone fracture healing: cell therapy in delayed unions and nonunions. Bone 2015;70:93–101. https://doi.org/10.1016/j.bone.2014.07.033.
[3] Hobby B, Lee MA. Managing atrophic nonunion in the geriatric population: incidence, distribution, and causes. Orthop Clin N Am 2013;44(2):251–6. https://doi.org/10.1016/j.ocl.2013.01.011.
[4] Megas P. Classification of non-union. Injury 2005;36(Suppl 4):S30–7. https://doi.org/10.1016/j.injury.2005.10.008.
[5] Rupp M, Biehl C, Budak M, Thormann U, Heiss C, Alt V. Diaphyseal long bone nonunions - types, aetiology, economics, and treatment recommendations. Int Orthop 2018;42(2):247–58. https://doi.org/10.1007/s00264-017-3734-5.
[6] Dimitriou R, Carr IM, West RM, Markham AF, Giannoudis PV. Genetic predisposition to fracture non-union: a case control study of a preliminary single nucleotide polymorphisms analysis of the BMP pathway. BMC Muscoskel Disord 2011;12:44. https://doi.org/10.1186/1471-2474-12-44.
[7] Calori GM, Albisetti W, Agus A, Iori S, Tagliabue L. Risk factors contributing to fracture non-unions. Injury 2007;38(Suppl 2):S11–8. https://doi.org/10.1016/s0020-1383(07)80004-0.
[8] Dickson K, Katzman S, Delgado E, Contreras D. Delayed unions and nonunions of open tibial fractures. Correlation with arteriography results. Clin Orthop Relat Res 1994;302:189–93.
[9] Reed AA, Joyner CJ, Brownlow HC, Simpson AH. Human atrophic fracture non-unions are not avascular. J Orthop Res 2002;20(3):593–9. https://doi.org/10.1016/s0736-0266(01)00142-5.
[10] Brownlow HC, Reed A, Simpson AH. The vascularity of atrophic non-unions. Injury 2002;33(2):145–50. https://doi.org/10.1016/s0020-1383(01)00153-x.
[11] Hernigou P, Poignard A, Beaujean F, Rouard H. Percutaneous autologous bone-marrow grafting for nonunions. Influence of the number and concentration of progenitor cells. J Bone Joint Surg Am 2005;87(7):1430–7. https://doi.org/10.2106/jbjs.D.02215.
[12] Tawonsawatruk T, Kelly M, Simpson H. Evaluation of native mesenchymal stem cells from bone marrow and local tissue in an atrophic nonunion model. Tissue Eng C Methods 2014;20(6):524–32. https://doi.org/10.1089/ten.TEC.2013.0465.
[13] Bajada S, Marshall MJ, Wright KT, Richardson JB, Johnson WE. Decreased osteogenesis, increased cell senescence and elevated Dickkopf-1 secretion in human fracture non union stromal cells. Bone 2009;45(4):726–35. https://doi.org/10.1016/j.bone.2009.06.015.
[14] Ismail HD, Phedy P, Kholinne E, Kusnadi Y, Sandhow L, Merlina M. Existence of mesenchymal stem cellsin sites of atrophic nonunion. Bone & joint research 2013;2(6):112–5. https://doi.org/10.1302/2046-3758.26.2000165.
[15] Orth M, Kruse NJ, Braun BJ, Scheuer C, Holstein JH, Khalil A, et al. BMP-2-coated mineral coated microparticles improve bone repair in atrophic non-unions. Eur Cell Mater 2017;33:1–12. https://doi.org/10.22203/eCM.v033a01.
[16] Risbud MV, Shapiro IM, Guttapalli A, Di Martino A, Danielson KG, Beiner JM, et al. Osteogenic potential of adult human stem cells of the lumbar vertebral body and the iliac crest. Spine 2006;31(1):83–9. https://doi.org/10.1097/01.brs.0000193891.71672.e4.
[17] Osugi M, Katagiri W, Yoshimi R, Inukai T, Hibi H, Ueda M. Conditioned media from mesenchymal stem cells enhanced bone regeneration in rat calvarial bone defects. Tissue Eng 2012;18(13–14):1479–89. https://doi.org/10.1089/ten.TEA.2011.0325.
[18] Dominici M, Le Blanc K, Mueller I, Slaper-Cortenbach I, Marini F, Krause D, et al. Minimal criteria for defining multipotent mesenchymal stromal cells. The International Society for Cellular Therapy position statement. Cytotherapy 2006;8(4):315–7. https://doi.org/10.1080/14653240600855905.
[19] Nicholson JA, Makaram N, Simpson A, Keating JF. Fracture nonunion in long bones: a literature review of risk factors and surgical management. Injury 2021;52(Suppl 2). S3–s11. https://doi.org/10.1016/j.injury.2020.11.029.
[20] Urist MR, Mazet Jr R, Mc LF. The pathogenesis and treatment of delayed union and non-union; a survey of eighty-five ununited fractures of the shaft of the tibia and one hundred control cases with similar injuries. J Bone Joint Surg Am 1954;36-a(5):931–80 [passim].
[21] Calori GM, Colombo M, Mazza E, Ripamonti C, Mazzola S, Marelli N, et al. Monotherapy vs. polytherapy in the treatment of forearm non-unions and bone defects. Injury 2013;44(Suppl 1):S63–9. https://doi.org/10.1016/s0020-1383(13)70015-9.
[22] Quacci D, Dell'Orbo C, Salvi M, Bartolozzi P, Misasi M. Ultrastructural aspects of human nonunion. Histol Histopathol 1991;6(1):87–93.
[23] Wildemann B, Ignatius A, Leung F, Taitsman LA, Smith RM, Pesántez R, et al. Non-union bone fractures. Nat Rev Dis Prim 2021;7(1):57. https://doi.org/10.1038/s41572-021-00289-8.
[24] Vallim FC, Guimarães JAM, Dias RB, Sartore RC, Cavalcanti ADS, Leal AC, et al. Atrophic nonunion stromal cells form bone and recreate the bone marrow environment in vivo. OTA Int 2018;1(3):e008. https://doi.org/10.1097/oi9.0000000000000008.
[25] Li SG, Huang Y, Zhu HJ, Huang JF. Percutaneous injection of platelet-rich plasma to treat atrophic nonunion after internal fixation of ulnar fracture: a case report. Nagoya J Med Sci 2021;83(1):201–8. https://doi.org/10.18999/nagjms.83.1.201.
[26] Leighton R, Watson JT, Giannoudis P, Papakostidis C, Harrison A, Steen RG. Healing of fracture nonunions treated with low-intensity pulsed ultrasound (LIPUS): a systematic review and meta-analysis. Injury 2017;48(7):1339–47. https://doi.org/10.1016/j.injury.2017.05.016.
[27] Cuthbert RJ, Jones E, Sanjurjo-Rodríguez C, Lotfy A, Ganguly P, Churchman SM, et al. Regulation of angiogenesis discriminates tissue resident MSCs from effective and defective osteogenic environments. J Clin Med 2020;9(6). https://doi.org/10.3390/jcm9061628.
[28] Takahara S, Niikura T, Lee SY, Iwakura T, Okumachi E, Kuroda R, et al. Human pseudoarthrosis tissue contains cells with osteogenic potential. Injury 2016;47(6):1184–90. https://doi.org/10.1016/j.injury.2016.02.022.
[29] Behrens A, van Deursen JM, Rudolph KL, Schumacher B. Impact of genomic damage and ageing on stem cell function. Nat Cell Biol 2014;16(3):201–7. https://doi.org/10.1038/ncb2928.
[30] Tang Y, Wu X, Lei W, Pang L, Wan C, Shi Z, et al. TGF-beta1-induced migration of bone mesenchymal stem cells couples bone resorption with formation. Nat Med 2009;15(7):757–65. https://doi.org/10.1038/nm.1979.
[31] Linkhart TA, Mohan S, Baylink DJ. Growth factors for bone growth and repair: IGF, TGF beta and BMP. Bone 1996;19(1 Suppl):1s–12s. https://doi.org/10.1016/s8756-3282(96)00138-x.
[32] Jann J, Gascon S, Roux S, Faucheux N. Influence of the TGF-β superfamily on osteoclasts/osteoblasts balance in physiological and pathological bone conditions. Int J Mol Sci 2020;21(20). https://doi.org/10.3390/ijms21207597.
[33] Xie H, Cui Z, Wang L, Xia Z, Hu Y, Xian L, et al. PDGF-BB secreted by preosteoclasts induces angiogenesis during coupling with osteogenesis. Nat Med 2014;20(11):1270–8. https://doi.org/10.1038/nm.3668.
[34] Lindsey RC, Rundle CH, Mohan S. Role of IGF1 and EFN-EPH signaling in skeletal metabolism. J Mol Endocrinol 2018;61(1). T87–t102. https://doi.org/10.1530/jme-17-0284.
[35] Ye F, Li J, Xu P, Xie Z, Zheng G, Liu W, et al. Osteogenic differentiation of mesenchymal stem cells promotes c-Jun-dependent secretion of interleukin 8 and mediates the migration and differentiation of CD4(+) T cells. Stem Cell Res Ther 2022;13(1):58. https://doi.org/10.1186/s13287-022-02735-0.
[36] Gulati GS, Murphy MP, Marecic O, Lopez M, Brewer RE, Koepke LS, et al. Isolation and functional assessment of mouse skeletal stem cell lineage. Nat Protoc 2018;13(6):1294–309. https://doi.org/10.1038/nprot.2018.041.
[37] Ravi M, Paramesh V, Kaviya SR, Anuradha E, Solomon FD. 3D cell culture systems: advantages and applications. J Cell Physiol 2015;230(1):16–26. https://doi.org/10.1002/jcp.24683.